IOPscience iopscience.iop.org

Home Search Collections Journals About Contact us My IOPscience

Structural and electronic properties of the triangular lattice system Na_xCoO_2

This article has been downloaded from IOPscience. Please scroll down to see the full text article.

2006 J. Phys.: Condens. Matter 18 8673

(http://iopscience.iop.org/0953-8984/18/37/023)

View the table of contents for this issue, or go to the journal homepage for more

Download details:
IP Address: 129.252.86.83
The article was downloaded on 28/05/2010 at 13:46

Please note that terms and conditions apply.

INSTITUTE OF PHYSICS PUBLISHING JOURNAL OF PHYSICS: CONDENSED MATTER

J. Phys.: Condens. Matter **18** (2006) 8673–8682 doi:10.1088/0953-8984/18/37/023

Structural and electronic properties of the triangular lattice system Na_xCoO_2

Tomohiro Ikeda and Masashige Onoda

Institute of Physics, University of Tsukuba, Tennodai, Tsukuba 305-8571, Japan

E-mail: onoda@sakura.cc.tsukuba.ac.jp

Received 27 June 2006, in final form 27 July 2006
Published 1 September 2006
Online at stacks.iop.org/JPhysCM/18/8673

Abstract

The structural and electronic properties of the triangular lattice system Na_xCoO_2 with nominal compositions of $0.7 \leqslant x \leqslant 1$ annealed at temperatures from 923 to 1123 K have been explored by means of x-ray diffraction and through measurements of electrical resistivity, thermoelectric power and magnetization. All of the properties for the single-phase specimens are classified into two groups according to the annealing temperature, and a significant correlation exists between the transport and magnetic properties. The first-order phase transition and the irreversible transition for the transport properties, likely due to the ordering of Na ions and to the metastability in the local structure for the polycrystalline specimens, respectively, are also pointed out.

1. Introduction

Transition-metal oxides and the ternary oxide bronzes exhibit a wide variety of structures and properties originated from the unique nature of partially filled d-bands. They have often been investigated from the viewpoints of electron correlation, electron–phonon coupling and quantum spin-fluctuation systems.

Frustrated quantum antiferromagnets with a low spin number $S = 1/2$ or 1 have been explored for a long time, since the proposal of resonating-valence-bond theory regarding a spin-liquid ground state for the Heisenberg-type interaction on the triangular lattice [1, 2]. For the spatially isotropic interactions, the ground state seems to show long-range magnetic order [3]. On the other hand, several characteristic ground states such as spin-trimer [4] and spin-ice [5] have been revealed.

The triangular lattice oxide system $Na_xCoO_2 \cdot yH_2O$ with $x \simeq 0.3$ and $y \simeq 1.3$ obtained with a soft-chemical method exhibits superconductivity at $T_c \simeq 5$ K [6], which has given rise to new interests in the research of geometrically frustrated oxide system. The parent compound system Na_xCoO_2 is also known to exhibit large thermoelectric power for a metal [7]. For this system, obtained by solid-state reaction, four different phases were reported previously [8]:

rhombohedral α for $0.9 \leqslant x \leqslant 1$; monoclinic α' for $x = 0.75$; orthorhombic β for $0.55 \leqslant x \leqslant 0.6$; and hexagonal γ for $Na_xCo_yO_2$ with $x < 1$, $y \leqslant 1$ and $0.55 \leqslant x/y \leqslant 0.74$. Subsequent structural studies including compounds prepared with the soft-chemical method and the flux one indicate that the space groups for the compositions with $x = 0.5, 0.67, 0.7$ and 1 are $Pnmm$ [9], $C2/m$ [10], $P6_3/mmc$ [11] and $R\bar{3}m$ [12]. The $P6_3/mmc$ phase has three kinds of structural model for the Na sites [13, 9]. Here it should be noted that the space group of Na_xCoO_2 depends not only on the concentration of Na but also on the preparation method.

This work is aimed at the γ-phase of Na_xCoO_2 having the same space group as that for the superconducting phase. The structure is basically described in terms of CoO_6 octahedra which are joined by sharing edges to form a two-dimensional triangular lattice of Co ions. Between these lattices, the Na atoms labelled Na1 and Na2 for 2b and 2d sites, respectively, with trigonal prismatic environment reside in some occupation probability. The space groups of the nonstoichiometric Na_xCoO_2 introduced above may be partly attributed to the difference of the occupation probability of Na that is likely related to the partial order of Co valence. Since the Na1–Na2 distance is significantly smaller than that expected from the ionic radius, these sites cannot be occupied simultaneously due to the strong Coulomb repulsion. This type of randomness may affect the electronic properties, as often seen in nonstoichiometric bronzes [14]. The Co–Na1 distance along the hexagonal c-direction is smaller than the Co–Co distance, which may also influence the electronic properties.

There are many reports regarding the electronic properties of γ-Na_xCoO_2, which may be classified into two groups: those with a magnetic anomaly at low temperatures [15–21] and those without it [22]. The former reports are further divided into those with a resistivity anomaly at around room temperature [15–17] and those without it [18–21]. The magnetic transition at low temperatures is attributed to the formation of spin-density-wave (SDW) or antiferromagnetic states, and the resistivity anomaly at high temperatures is attributed to the ordering in the Na layers. As regards the thermoelectric power, the large magnitude is explained in terms of the spin entropy of the carriers [22, 23] or the Boltzmann transport equation with the electronic structure determined by the photoemission measurement [24], as will be described later.

To date there have been few reports on how the structural and electronic properties vary with the annealing temperature in spite of intensive studies as introduced above. According to this temperature, the chemical composition as well as the detail of the crystal structure is expected to change. In this work, the Na_xCoO_2 system with nominal compositions of $0.7 \leqslant x \leqslant 1$ has been prepared at various annealing temperatures as described in section 2. The structural characteristics explored by means of x-ray powder diffraction are described in section 3.1, and the transport and magnetic properties revealed through measurements of electrical resistivity, thermoelectric power and magnetization for the single-phase specimens are discussed in sections 3.2 and 3.3, respectively. Section 4 is devoted to conclusions.

2. Experiments

Polycrystalline specimens of Na_xCoO_2 with nominal x values of 0.7, 0.8, 0.9 and 1 were prepared by the solid-state reaction method. Appropriate mixtures of Na_2CO_3 dried at 473 K and Co_3O_4 (99.99% purity) were put in an electric furnace kept at temperatures of $T_a = 923, 973, 1023, 1073$ and 1123 K in air and they were annealed for 18 h, and then quenched to room temperature. These specimens are referred to as (I). Specimens with Na_2CO_3 and Co_3O_4 dried at 573 K, hereafter called (II), were also made.

Inductively coupled plasma-optical emission spectroscopy (ICP) and x-ray powder diffraction were performed on the prepared specimens at room temperature using a Nippon

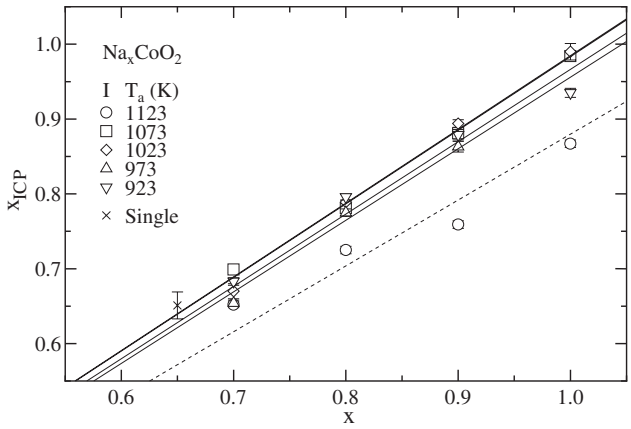

Figure 1. The relation between the nominal Na concentrations and the ICP values for Na_xCoO_2 (I) annealed at $T_a = 923$–1123 K, where the full and dotted lines indicate the linear fits of $x_{ICP} \propto x$. The result for the single crystals [25] is plotted for comparison.

Jarrell-Ash ICAP-575 spectrometer and a Rigaku RAD-IIC diffractometer with Cu Kα radiation, respectively. For (II), no ICP analysis was done because of trouble with the spectrometer. The four-terminal electrical resistivity and thermoelectric power were measured with a dc method at temperatures from 4.2 to 320 K at the typical cooling rates of 1 and 0.5 K min^{-1}, respectively. The magnetizations were measured on heating at temperatures between 4.2 and 300 K by the Faraday method with a field of up to 1 T, where the temperature was first quenched to 4.2 K. The magnetic susceptibility was deduced from the linear part of the magnetization–field (M–H) curve with a decreasing field and the remanent magnetization was obtained from the intercept.

3. Results and discussions

3.1. Structural properties

The composition with $x = 0.7$ (I, II) has a small amount of Co_3O_4 as a second phase, while those from 0.8 to 1 exhibit a powder diffraction pattern similar to that of the averaged cell calculated on the basis of the atomic parameters determined from the single-crystal diffraction of $Na_{0.65}CoO_2$ [25] irrespective of the annealing temperature. This single γ-phase corresponds to the H2 phase in the terminology adopted previously [13, 9], although our structural study for $Na_{0.65}CoO_2$ [25] provides a result different from the previous one [13, 9].

The Na concentration per Co ion for (I) estimated by ICP, x_{ICP}, is plotted in figure 1 as a function of the nominal value x. For the specimens annealed at $T_a = 923$–1073 K, x_{ICP} is described by $x_{ICP} = (0.96$–$0.98)x$ as shown by the full lines, and for those annealed at $T_a = 1123$ K, $x_{ICP} = 0.88x$. Thus, it may be concluded that the actual concentration of Na for (I) is smaller than the nominal value. In particular, the annealing at 1123 K gives rise to a relatively large deficiency of Na ions. Nevertheless, in this work, the nominal compositions will be used, since the experimental data are not simply classified with x_{ICP} alone.

Figure 2 shows the x-dependences of the lattice constants at room temperature. The data for (I) are roughly classified into two groups as indicated by the dotted and full curves; one group is the results for the specimens annealed at $T_a \leqslant 973$ K and the other is for $T_a \geqslant 1023$ K. That is, the annealing temperature with which the composition dependences are classified T_{ac}

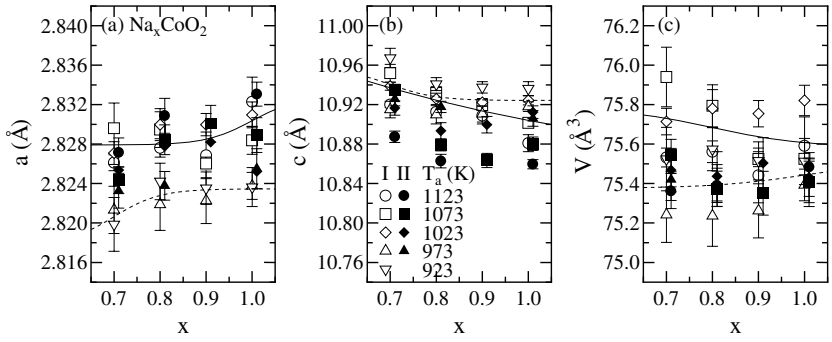

Figure 2. The nominal composition dependences of the hexagonal lattice constants: (a) a; (b) c; and (c) V for the polycrystalline specimens of Na_xCoO_2 (I, II) annealed at $T_a = 923$–1123 K. Here, the dotted and full curves in (a)–(c) are guides for eyes regarding the results for (I) at $T_a \leqslant 973$ K and at $T_a \geqslant 1023$ K, respectively.

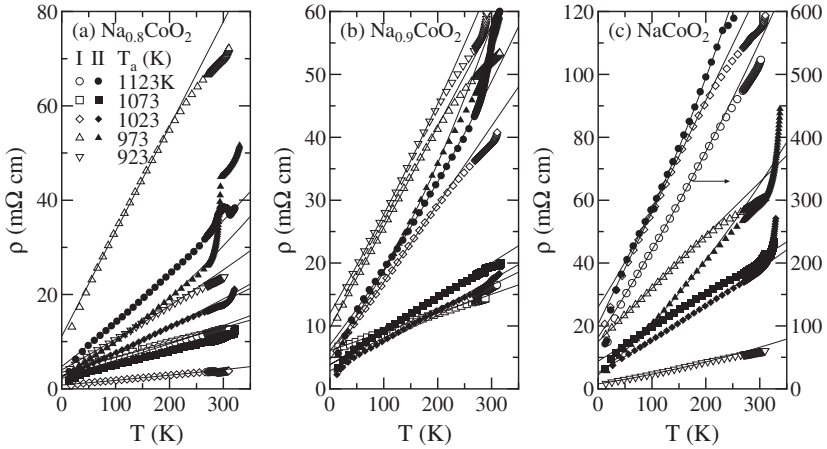

Figure 3. The temperature dependences of the electrical resistivities for the polycrystalline specimens of Na_xCoO_2 (I, II) annealed at $T_a = 923$–1123 K: (a) $x = 0.8$; (b) $x = 0.9$; and (c) $x = 1$. All of the full lines and curves denote fits to equation (1).

ranges from 973 to 1023 K. For the single-phase region at $T_a < T_{ac}$, the lattice constants change little with x. On the other hand, for $T_a > T_{ac}$, a increases slightly, and c and the volume V decrease. In addition, a and V for $T_a < T_{ac}$ are smaller than those for $T_a > T_{ac}$, while c indicates an opposite behaviour. The x-dependence of a for (II) is qualitatively similar to that for (I), whereas c has a smaller value. The annealing at high temperatures leads to the increase of a, which may correspond to the increase of ionic radius of Co when the z-coordinate of the O ion does not change significantly. Thus, the number of Co^{4+} ions for the compound annealed at high temperatures is expected to be enhanced as compared with that at low temperatures.

3.2. Transport properties

3.2.1. Electrical resistivity. The results for the composition with $x = 0.7$ that has the impurity phase of Co_3O_4 are not described below. The temperature dependences of the electrical resistivities ρ with $x = 0.8$, 0.9 and 1 in the heated process are shown in figures 3(a)–(c),

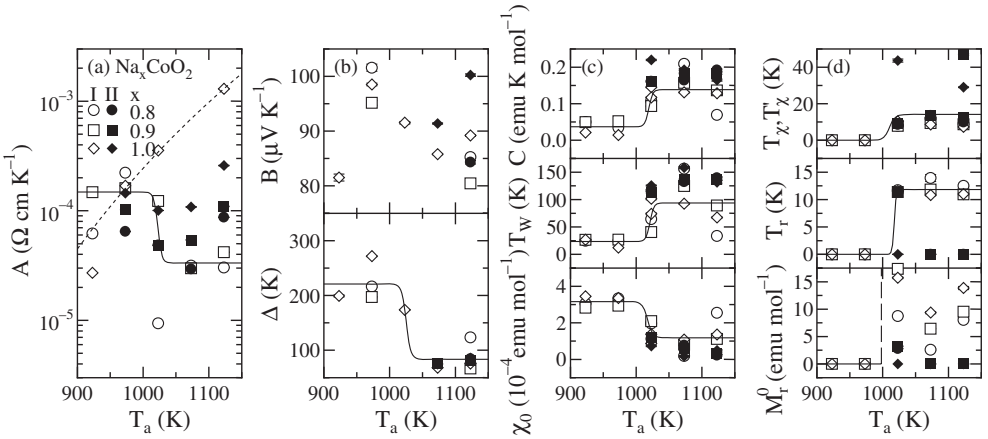

Figure 4. The annealing temperature dependences of the physical parameters for Na_xCoO_2 (I, II) with $x = 0.8$, 0.9 and 1: (a) equation (1) for the electrical resistivities; (b) equation (2) for the thermoelectric powers; (c) equation (3) for the magnetic susceptibilities at high temperatures; and (d) equation (4) for the remanent magnetizations and the temperature at which the susceptibility has a peak. All of the curves are guides for eyes.

respectively. Although the Mott-type variable-range hopping (VRH) transport would appear to be due to the effect of nonstoichiometry or randomness of Na ions [26], especially for the composition near to band insulator $NaCoO_2$, all of the specimens indicate metallic conductions. The data are approximately linear with temperature between 50 and 200 K. According to the equation,

$$\rho = \rho_0 + AT + A'T^2 \tag{1}$$

where ρ_0 is a residual resistivity, and A and A' are constants, the annealing temperature dependence of A is obtained as shown in figure 4(a) on the basis of the full lines and curves in figure 3. Here the contribution from the third term is significantly small as compared with that from the second term. The A values have a tendency to increase with increasing x. The results for $x = 0.8$ and 0.9 (I) may be classified with T_{ac}; A for $T_a < T_{ac}$ is larger than that for $T_a > T_{ac}$. For (II), on the other hand, there is no clear boundary.

Between 200 K and room temperature, the temperature dependences of the resistivities often exhibit anomalies or a significant deviation from the full curves of equation (1), as shown in figure 3. In order to characterize this anomaly, systematic measurements on the thermal variations of the resistivities for (II) were made with the conditions of slow cooling (SC) and fast cooling (FC) rates of 0.5 and 5 K min^{-1}, respectively. Figure 5(a) shows the results for $x = 0.8$, 0.9 and 1.0 (II). The SC data of (II) clearly exhibit first-order phase transitions at around room temperature. The FC data also indicate first-order transitions for the initial cooled process. However, for the heated process with FC, the irreversible transitions appear at a temperature slightly lower than the first-order transition temperature on heating with SC. This first-order transition for the resistivity, which has often been observed in the nonstoichiometric vanadium bronzes [14], may be attributed to the random potential effect of Na ions. Here it is noted that the first-order transition in Na_xCoO_2 occurs irrespective of the present cooling condition, whereas in the vanadium bronzes it is predominant for the SC process.

In order to clarify the irreversible transition for the FC data of the resistivity, further measurements were performed with the FC condition as follows. First, the temperature was lowered to a certain temperature T_L, and raised to about 320 K, and then it decreased to a

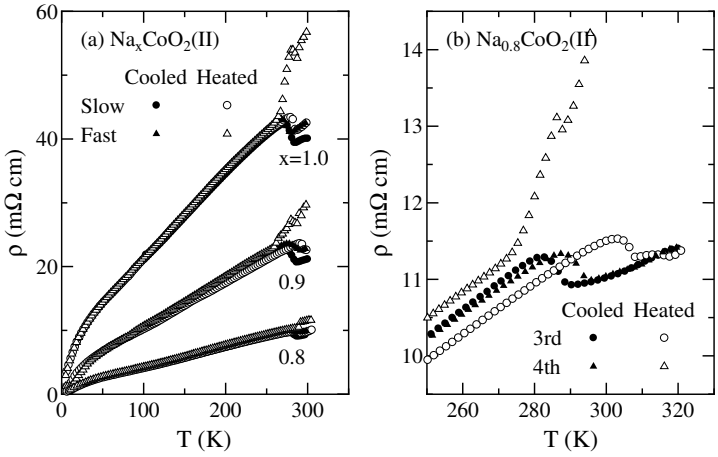

Figure 5. The temperature dependences of the electrical resistivities for polycrystalline specimens of Na_xCoO_2 (II) annealed at $T_a = 1073$ K: (a) the data for $x = 0.8$, 0.9 and 1 in SC and FC conditions; and (b) the data for $x = 0.8$ in the FC condition with $T_L = 168$ and 158 K for the third and fourth cycles, respectively.

temperature lower than the initial T_L. Figure 5(b) indicates the thermal cycles of the resistivity for $x = 0.8$ (II), where $T_L = 168$ and 158 K for the third and fourth cycles, respectively. A slight difference of the first-order transition temperature on cooling may be inevitable for the present condition of measurement. When $T_L \geqslant 168$ K, only the first-order phase transition appears between 280 and 310 K, as described above. In contrast, for $T_L \leqslant 158$ K, the resistivity has the irreversible transition at about 270 K. Thus, the FC state below 158 K is metastable, likely due to the local structural change governed by the temperature given by the present experimental condition.

At temperatures below 50 K, the resistivities become smaller than the values expected from equation (1), which is notable for (II).

3.2.2. Thermoelectric power. Figures 6(a)–(c) show the temperature dependences of the thermoelectric powers S with $x = 0.8$, 0.9 and 1 (I, II) on heating, respectively. The data are positive except for the low-temperature region for $x = 0.8$ (I), indicating that the carriers are holes. As the nominal composition increases, the thermoelectric power has a tendency to increase. Around room temperature where the first-order transition of the resistivity appears, the thermoelectric power also exhibits an anomaly. The present condition of the thermoelectric power measurement does not give rise to the irreversible transition.

At temperatures between 250 and 50 K, all of the data indicate upward curvatures approximately expressed as

$$S = S_0 + B\exp(-\Delta/T) \tag{2}$$

where S_0 is a constant close to zero and Δ is the apparent energy gap. Figure 4(b) shows the annealing temperature dependences of B and Δ. This kind of temperature dependence may be understood by considering the conductivity-weighted mean for the two types of carrier. In effect, Na_xCoO_2 has two a_{1g} and four e_g symmetry bands in the rhombohedral crystal field, so two kinds of carrier having these characters likely contribute to the conduction. Here the anisotropic resistivity is assumed to have a similar temperature dependence. One carrier is metallic with small S_m and large conductivity $\sigma_m \propto 1/T$, and the other carrier has a

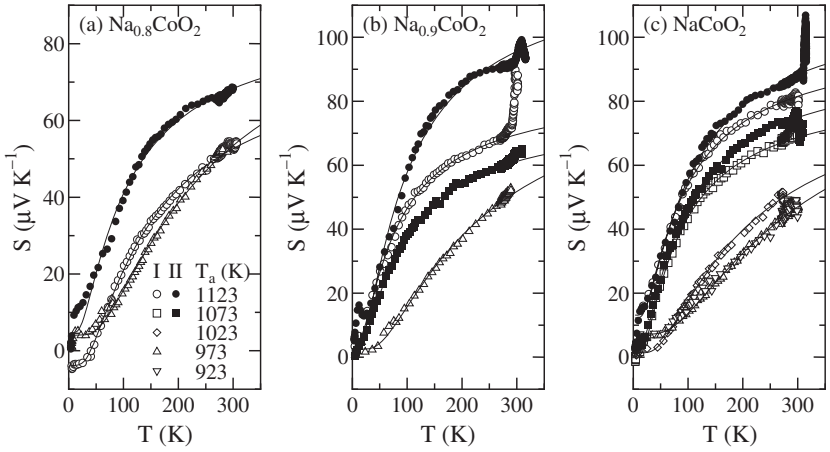

Figure 6. The temperature dependences of the thermoelectric powers for the polycrystalline specimens of Na_xCoO_2 (I, II) annealed at $T_a = 923$–1123 K: (a) $x = 0.8$; (b) $x = 0.9$; and (c) $x = 1$. All of the full curves indicate fits to equation (2).

semiconducting behaviour with $S_s \propto 1/T$ and activation-type conductivity $\sigma_s \propto \exp(-\Delta/T)$. B ranges from 80 to 100 μV K^{-1}. Considering the inevitable deficiency of Na ions in this system, it is noted that these values are not so different from those of the Heikes formula in the high-temperature limit [27]; $S_H = (k/e)\ln[(2-x)/x]$, where k is the Boltzmann coefficient. Δ has a clear boundary regarding T_a; $\Delta \approx 220$ and 80 K for the specimens prepared below and above T_{ac}, respectively. The reason why the classification according to T_a for the thermoelectric power data is distinct as compared with that for the electrical resistivity data is that the effect of grain-boundary resistance for the former data is less significant.

As introduced in section 1, the large magnitude and the suppression in the presence of magnetic field of the thermoelectric power have been interpreted to arise from spin entropy of the carriers [22, 23]. In addition, it is pointed out that for strongly correlated electron systems with orbital degeneracy, the resistivity is not much affected by the degeneracy [23]. An alternative analysis estimated on the basis of the Boltzmann transport equation with the electronic structure determined by photoemission measurement is reported to account for the experimental results for a certain composition [24]. In order to judge which of these models including the simple two-carrier case is more appropriate, further experiments and considerations are necessary.

At temperatures below 50 K, the data for (I) are almost constant as fitted with equation (2), while those for (II) indicate a small hump. This anomaly and the resistivity one may be related to a long-range magnetic order, as will be discussed in the next section.

3.3. Magnetic properties

The inverse magnetic susceptibilities χ^{-1} with $x = 0.8$, 0.9 and 1 as a function of temperature are shown in figures 7(a)–(c), respectively. At the high-temperature side, none of the susceptibility data indicate any anomaly, which is a striking contrast to the transport properties in section 3.2. They increase with decreasing temperature and apparently follow a Curie–Weiss law,

$$\chi = \frac{C}{T + T_W} + \chi_0 \tag{3}$$

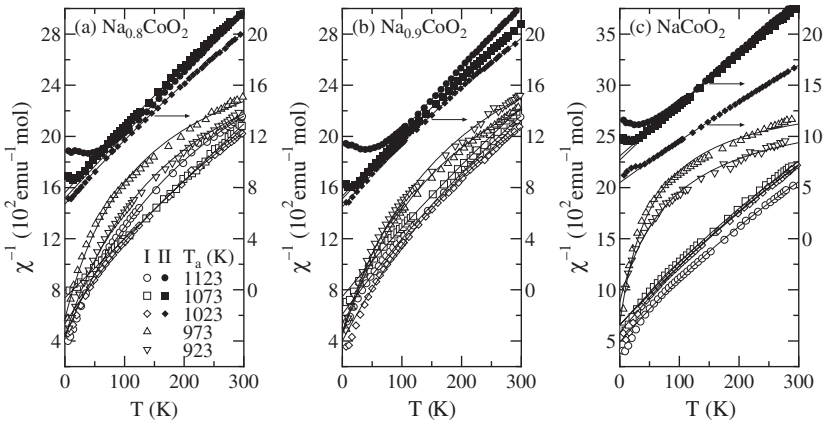

Figure 7. The temperature dependences of the inverse magnetic susceptibilities for polycrystalline specimens of Na_xCoO_2 (I, II) annealed at $T_a = 923$–1123 K: (a) $x = 0.8$; (b) $x = 0.9$; and (c) $x = 1$. All of the full curves are fits to equation (3).

where C is the Curie constant, T_W is the Weiss temperature and χ_0 corresponds to the temperature-independent susceptibility of the Van Vleck orbital and diamagnetic components. According to some cases, the Pauli paramagnetic contribution is approximately included in χ_0. The results of C, T_W and χ_0 obtained by fitting equation (3) to the data are shown in figure 4(c). Since the ideal composition of $x' = 1$ with space group $P6_3/mmc$ is considered to be a band insulator made of filled-shell nonmagnetic Co^{3+}, the composition dependence of the Curie constant on the basis of a localized electron model is given by $C \simeq 0.38x$ with the assumption of $g \approx 2$. Taking account of the Na deficiency described in section 3.1, the results for the specimens prepared below T_{ac} may be explained in terms of this model with $T_W \approx 30$ K and $\chi_0 \approx 3 \times 10^{-4}$ emu mol^{-1}. Above T_{ac}, in contrast, C roughly corresponds to the value for $x' = 0.7$ irrespective of x, where $T_W \approx 10^2$ K and $\chi_0 \approx 1 \times 10^{-4}$ emu mol^{-1}. From these results, the specimens prepared above T_{ac} are found to be more magnetic and to have a larger exchange constant. In order to discuss these differences for the magnetic parameters according to the annealing temperature, it is necessary to know the *precise* chemical formula, since the deficiencies of Na and Co ions with the type of $Na_{x-\delta}Co_{1-\delta'}O_2$ give rise to unpaired electrons even when the ratio Na/Co is unity.

The low-temperature behaviours also depend on the annealing temperature. For the specimens annealed below T_{ac}, there seems *no anomaly*. On the other hand, for those annealed above T_{ac}, the susceptibility has *a peak* at $T_\chi \approx 10$–20 K as plotted in the top panel of figure 4(d). A part of (II) have an additional broad peak around $T'_\chi \approx 40$ K. It should be noted that the susceptibility for a spin-1/2 Heisenberg antiferromagnet on a triangular lattice exhibits a maximum at $T \simeq T_W/4$ [28]. This relation seems to be valid for the specimens with T'_χ.

For (I) having a finite T_χ and a part of (II), the remanent magnetizations M_r appear as shown in figure 8. Except for the short-range order region where the remanent magnetization exhibits downward curvatures, the temperature dependence is approximated with the order parameter exponent of unity:

$$M_r = M_r^0(1 - T/T_r) \tag{4}$$

where M_r^0 is the remanent magnetization at $T = 0$ K and T_r is the transition temperature. The bottom and middle panels of figure 4(d) indicate the annealing temperature dependences of M_r^0

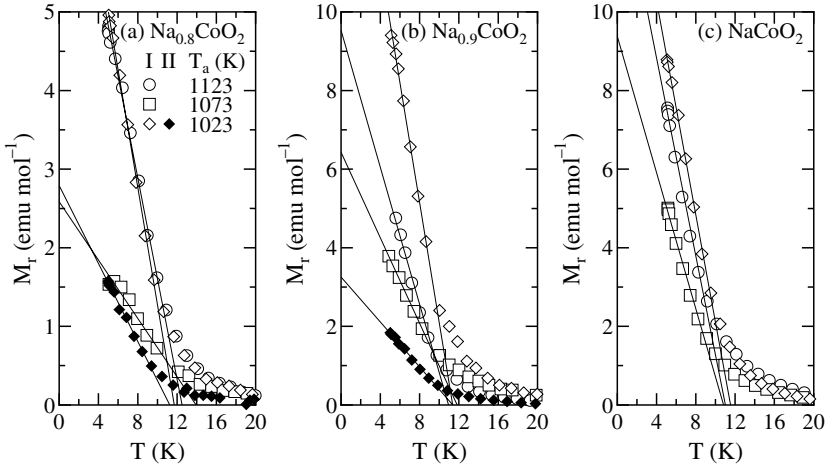

Figure 8. The temperature dependences of the remanent magnetizations for polycrystalline specimens of Na_xCoO_2 (I, II) annealed at $T_a = 923$–1123 K: (a) $x = 0.8$; (b) $x = 0.9$; and (c) $x = 1$. All of the full curves indicate fits to equation (4).

and T_r, respectively. The magnitude of M_r^0 corresponds to the order of $10^{-3}\mu_B$ and T_r agrees roughly with T_χ. These results are consistent with the previous conclusion that the SDW or antiferromagnetic transition occurs at around $T_\chi \approx T_r$ [15–21], although it is reported that, in some cases, polycrystalline specimens have no transition. The remanent magnetization may be attributed to the canting of the antiferromagnetic states. For the localized electron system, the so-called frustration parameter is defined as the ratio of T_W to $T_\chi \approx T_r$. Applying this definition to the results for the metallic specimens annealed above T_{ac}, the parameters range from 5 to 10.

4. Conclusions

The structural and electronic properties of the triangular lattice system Na_xCoO_2 with nominal compositions of $0.7 \leqslant x \leqslant 1$ annealed at temperatures from 923 to 1123 K have been investigated. According to the annealing temperature, these properties for the single-phase specimens vary significantly, since the chemical composition as well as the local structure is modified. The overall temperature dependences of thermoelectric power are approximately explained with the two-carrier model and those of magnetic susceptibility at high temperatures are fitted with the Curie–Weiss law. The specimens annealed below T_{ac} that ranges from 973 to 1023 K have an enhanced gap for the poor metallic carriers and they are less magnetic, having a Curie constant almost consistent with the localized electron model. On the other hand, above T_{ac}, the apparent gap of poor metallic carriers is reduced significantly, the Curie–Weiss parameters are enhanced, and an antiferromagnetic or SDW-like transition takes place. At this transition temperature, the resistivity becomes smaller than the value extrapolated from the high-temperature side and the thermoelectric power exhibits a hump. The fact that the metallic state is preserved for this temperature region does not contradict the present two-carrier model. Alternatively, Na_xCoO_2 is considered to be located near the boundary between the antiferromagnetic metal and the correlated metal as in the case of the perovskite system $La_{1-x}Sr_xTiO_3$ with $x \approx 0.05$ [29]. It should be noted that many of the investigations performed to date are for specimens annealed above T_{ac}. In order to clarify the properties

of the present system completely, it is essential to know the absolute chemical composition of $Na_{x-\delta}Co_{1-\delta'}O_2$.

The first-order phase transitions of the electrical resistivities are observed irrespective of the present cooling condition, which may be due to the ordering of Na ions as described above. Since the susceptibility data do not exhibit any transition at the corresponding temperature, the resistivity anomaly is purely related to the charge dynamics. In addition, the irreversible transitions in the heated process are detected with the fast cooling down to a certain temperature. Our recent study on single-crystal specimens with $0.47 \leqslant x \leqslant 0.65$, outside of the composition for the present specimens, does not exhibit these transitions at temperatures below room temperature [25]. The difference in the resistivity anomalies may be due to the metastability in the local structure of the polycrystalline specimens rather than a difference of composition, which should be revealed from a microscopic point of view.

References

[1] Anderson P W 1973 *Mater. Res. Bull.* **8** 153
[2] Fazekas P and Anderson P W 1974 *Phil. Mag.* **30** 423
[3] See, for example Farnell D J J, Bishop R F and Gernoth K A 2001 *Phys. Rev.* B **63** 220402
[4] Onoda M, Naka T and Nagasawa H 1991 *J. Phys. Soc. Japan* **60** 2550
[5] Bramwell S T and Harris M J 1998 *J. Phys.: Condens. Matter* **10** L215
[6] Takada K, Sakurai H, Takayama-Muromachi E, Izumi F, Dilanian R A and Sakaki T 2003 *Nature* **422** 53
[7] Terasaki I, Sasago Y and Uchinokura K 1997 *Phys. Rev.* B **56** R12685
[8] Fouassier C, Matejka G, Reau J-M and Hagenmuller P 1973 *J. Solid State Chem.* **6** 532
[9] Huang Q, Foo M L, Lynn J W, Zandbergen H W, Lawes G, Wang Y, Toby B H, Ramirez A P, Ong N P and Cava R J 2004 *J. Phys.: Condens. Matter* **16** 5803
[10] Ono Y, Ishikawa R, Miyazaki Y, Ishii Y, Morii Y and Kajitani T 2002 *J. Solid State Chem.* **177** 177
[11] Balsys R J and Davis R L 1996 *Solid State Ion.* **93** 279
[12] Takahashi Y, Gotoh Y and Akimoto J 2003 *J. Solid State Chem.* **172** 22
[13] Huang Q, Khaykovich B, Chou F C, Cho J H, Lynn J W and Lee Y S 2004 *Phys. Rev.* B **70** 134115
[14] Onoda M and Hasegawa J 2006 *J. Phys.: Condens. Matter* **18** 2109
[15] Sales B C, Jin R, Affholter K A, Khalifah P, Veith G M and Mandrus D 2004 *Phys. Rev.* B **70** 174419
[16] Ihara Y, Ishida K, Michioka C, Kato M, Yoshimura K, Sakurai H and Takayama-Muromachi E 2004 *J. Phys. Soc. Japan* **73** 2963
[17] Wooldridge J, Paul D M K, Balakrishnan G and Lees M R 2005 *J. Phys.: Condens. Matter* **17** 707
[18] Bayrakci S P, Mirebeau I, Bourges P, Sidis Y, Enderle M, Mesot J, Chen D P, Lin C T and Keimer B 2005 *Phys. Rev. Lett.* **94** 157205
[19] Foo M L, Wang Y, Watauchi S, Zandbergen, He T, Cava R J and Ong N P 2004 *Phys. Rev. Lett.* **92** 247001
[20] Sakurai H, Tsuji N and Takayama-Muromachi E 2004 *J. Phys. Soc. Japan* **73** 2393
[21] Luo J L, Wang N L, Liu G T, Wu D, Jing X N, Hu F and Xiang T 2004 *Phys. Rev. Lett.* **93** 187203
[22] Wang Y, Ronado N S, Cava R J and Ong N P 2003 *Nature* **423** 425
[23] Koshibae W and Maekawa S 2001 *Phys. Rev. Lett.* **87** 236603
[24] Takeuchi T, Kondo T, Takami T, Takahashi H, Ikuta H, Mizutani U, Soda K, Funahashi R, Shikano M, Mikami M, Tsuda S, Yokoya T, Shin S and Muro T 2004 *Phys. Rev.* B **69** 125410
[25] Onoda M and Ikeda T, unpublished results (The single crystal of $Na_{0.65}CoO_2$ has a superlattice cell with $a_s = 2a$ and $c_s = c$ against the conventional hexagonal lattice constants a and c)
[26] Mott N F 1968 *J. Non-Cryst. Solids* **1** 1
[27] Heikes R R 1961 *Thermoelectricity* ed R R Heikes and R W Ure (New York: Interscience)
[28] Elstner N, Singh R R P and Young A P 1993 *Phys. Rev. Lett.* **71** 1629
[29] Onoda M and Kohno M 1998 *J. Phys.: Condens. Matter* **10** 1003